Quantum Dots

Deutsche Ausgabe: DOI: 10.1002/ange.201608019
Internationale Ausgabe: DOI: 10.1002/anie.201608019

# Thiolate-Mediated Photoinduced Synthesis of Ultrafine $Ag_2S$ Quantum Dots from Silver Nanoparticles

*Yitao Cao[+], Wei Geng[+], Run Shi, Lu Shang, Geoffrey I. N. Waterhouse, Limin Liu, Li-Zhu Wu, Chen-Ho Tung, Yadong Yin, and Tierui Zhang**

***Abstract:*** *Photoinduced syntheses offer significant advantages over conventional thermal strategies, including improved control over reaction kinetics and low synthesis temperatures, affording nanoparticles with nontrivial and thermodynamically unstable structures. However, the photoinduced syntheses of non-metallic nanocrystalline products (such as metal sulfides) have not yet been reported. Herein, we demonstrate the first photoinduced synthesis of ultrafine (sub-2 nm) $Ag_2S$ quantum dots (QDs) from Ag nanoparticles at 10°C. By thorough investigation of the mechanism for the transformation, a fundamental link was established between the intrinsic structures of the molecular intermediates and the final $Ag_2S$ products. Our results confirm the viability of low-temperature photochemical approaches in metal sulfide synthesis, and demonstrate a new rule which could be followed in it.*

The photosensitivity of silver compounds has been recognized for hundreds of years,[1] though research interest in silver in the past few decades has shifted increasingly towards silver nanoparticles and nanocrystalline silver compounds[2] which find applications in many areas including biosensing,[3] catalysis,[4] and imaging.[5] The interaction of light with silver nanoparticles generates intense localized surface plasmon resonances at visible wavelengths, the origin of which is now very well understood.[1,2] However, the light-sensitivity of Ag nanoparticles is generally not well understood. Jin et al. reported the photochemical conversion of Ag nanospheres to nanoprisms in 2001.[6] This pioneering study demonstrated a new photoinduced transformation of simple metal nanoparticles to synthesize nontrivial metallic nanostructures. Photoinduced syntheses offer many potential advantages over conventional thermal strategies employed in nanoparticle syntheses, including improved control over reaction kinetics and low synthesis temperatures.[7] Such control could permit the synthesis of nanomaterials with non-thermodynamically stable structures.[6–8] However, the photoinduced syntheses of non-metallic nanocrystalline products has not yet been reported.

For the synthesis of silver-based nanoparticles, a feasible strategy to realize this goal is to anchor the $Ag^+$ ion formed in initial stage of reaction and prevent its subsequent reduction as occurs in the ion-mediated sphere-to-prism pathway.[7b,c] Here, by introducing the aromatic thiol 4-*tert*-butylbenzenethiol (TBBT), we demonstrate for the first time a photoinduced synthesis of ultrafine (sub-2 nm) $Ag_2S$ quantum dots (QDs) from metallic Ag nanoparticles in nonpolar solvents at 10°C. Further, the synthesis is shown to follow a very distinctive Ag thiolate-mediated pathway. As illustrated in Scheme 1, the reaction is mediated by two forms of Ag

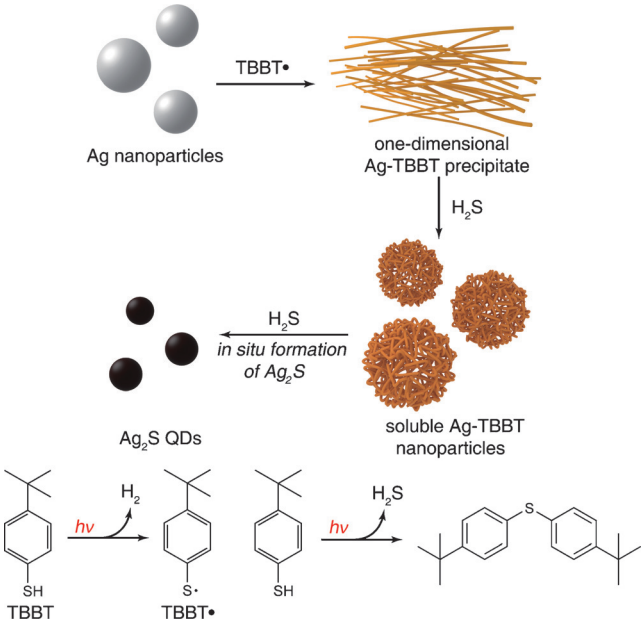


***Scheme 1.*** Illustration of the transformation from Ag nanoparticles to $Ag_2S$ QDs. The two reactions shown below demonstrate the photoinduced formation of thiol radicals (TBBT•) and $H_2S$ from excess TBBT.

thiolate, Ag–TBBT precipitate (insoluble Ag thiolate) and Ag–TBBT nanoparticles (soluble Ag thiolate). During the initial stage of reaction, TBBT is activated by light to form TBBT radicals, which etch the Ag nanoparticles to form an insoluble Ag-TBBT precipitate, which adopts a one-dimensional (1D) structure. The 1D Ag–TBBT precipitate decomposes and dissolves to form soluble Ag–TBBT nanoparticles through reaction with $H_2S$ released by the photoreaction of TBBT. The Ag–TBBT nanoparticles react with $H_2S$ to form $Ag_2S$ QDs in situ subsequently. Such ultrafine and monodisperse $Ag_2S$ QDs cannot be obtained by conventional thermal synthetic approaches, highlighting the merit of the low-temperature photochemical approach described here.

In a typical experiment, an excess amount of TBBT (0.30 mL, 1.80 mmol) was added to 6.0 mL of toluene containing 3.0 mg of 1-dodecanethiol-stabilized Ag nanoparticles (size: $3.5 \pm 1.2$ nm) synthesized through a two-phase

[*] Y. Cao,[+] R. Shi, Dr. L. Shang, Prof. L.-Z. Wu, Prof. C.-H. Tung, Prof. T. Zhang
Key Laboratory of Photochemical Conversion and Optoelectronic Materials
Technical Institute of Physics and Chemistry
Chinese Academy of Sciences
Beijing 100190 (China)
E-mail: tierui@mail.ipc.ac.cn
Dr. W. Geng,[+] Prof. L. Liu
Beijing Computational Science Research Center
Beijing 100084 (China)
Y. Cao,[+] R. Shi
University of Chinese Academy of Sciences
Beijing 100049 (China)
Prof. Y. Yin
Department of Chemistry
University of California, Riverside
California 92521 (USA)
Prof. G. I. N. Waterhouse
School of Chemical Sciences
The University of Auckland
Auckland 1142 (New Zealand)
[+] These authors contributed equally to this work.
Supporting information and the ORCID identification number(s) for the author(s) of this article can be found under http://dx.doi.org/10.1002/anie.201608019.

  

approach (Figure S1), followed by irradiation at 10 °C (see the Supporting Information for more details). As shown in Figure 1 a, the dark red color of the Ag nanoparticle solution faded quickly over a 30 min period. At longer reaction times,

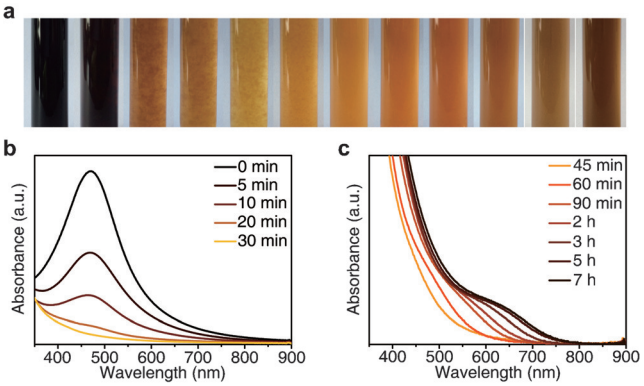


***Figure 1.*** a) Photographs of the reaction system during the course of the reaction. Time-dependent UV/Vis spectra b) from 0 min to 30 min and c) from 45 min to 7 h. The UV/Vis spectra were divided into two plots to show the absorption signal evolution more clearly.

a light yellow precipitate formed and then dissolved again to yield an orange solution, which progressively darkened during the course of reaction. Time-dependent UV/Vis spectroscopy was applied to follow the absorption changes of the reaction mixture during this process. Figure 1 b shows that the characteristic plasmon absorption peak of the Ag nanoparticles weakens and disappears over the first 30 min, indicating the total consumption of the Ag nanoparticles. Over the next few hours, a continuous red shift in the absorption signal was observed (Figure 1 c). This red shift ceased at prolonged reaction times (7 h, Figure S2), indicating termination of the reaction.

Following removal of the solvent and by-products, a black solid product was isolated which could be readily dispersed in nonpolar solvents. Transmission electron microscopy (TEM) showed that the reaction product comprised ultrafine nanoparticles of diameter $1.7 \pm 0.2$ nm (Figure 2 a), which were shown to be $Ag_2S$ QDs by further characterization studies (Figure S3). These $Ag_2S$ QDs remained stable for more than 10 months (Figure S4). Figure 2 b examines the optical properties of the ultrafine $Ag_2S$ QDs. A band gap of 1.47 eV was determined for the $Ag_2S$ QDs, blue-shifted considerably compared to the band gap determined for bulk monoclinic α-$Ag_2S$ (1.1 eV). The larger band gap determined for $Ag_2S$ QDs reflects the influence of quantum confinement. Furthermore, the photoluminescence emission peak of the $Ag_2S$ QDs is located at 820 nm, a wavelength also blue-shifted compared to literature reports for $Ag_2S$ QDs with larger particle sizes.[9a,b] The near-infrared emission characteristic of non-toxic monoclinic α-$Ag_2S$ QDs is an important property for their application as bioimaging probes.[9b–f]

Owing to the low $K_{sp}$ of most metal sulfides ($6.3 \times 10^{-50}$ at 25 °C for $Ag_2S$), reaction conditions for the synthesis of metal sulfide QDs need to be carefully controlled to avoid the formation of large-sized particles or unwanted nanocrystal-

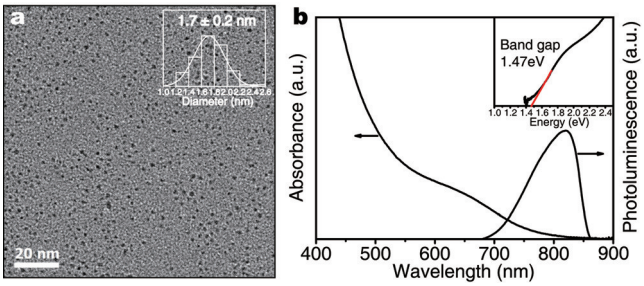


***Figure 2.*** a) TEM image of $Ag_2S$ QDs. Inset displays a particle size histogram for the $Ag_2S$ QDs and corresponding Gaussian fit. b) Absorption and photoluminescence spectra of $Ag_2S$ QDs (solvent: toluene). Inset shows the calculation of band gap with the Kubelka–Munk function. The abrupt drop of photoluminescence intensity at 850 nm is due to the limited detecting range of PMT detector, resulting in asymmetry of the curve, but the peak position is accurate.

line precipitates. High-quality metal sulfide QDs are typically synthesized at high temperatures, wherein a very brief nucleation is followed almost immediately by rapid growth.[9b,10] In contrast, the synthesis of $Ag_2S$ QDs described here took place at 10 °C with no discrete nucleation period, as evidenced by the slow reaction progress seen visually and by UV/Vis spectroscopy (Figure 1). These results suggest that a new and alternative reaction mechanism is responsible for producing the $Ag_2S$ QDs, which motivated a detailed investigation. Time-resolved UV/Vis spectra (Figure 1 b and c) revealed two distinct stages during the course of reaction: etching of Ag nanoparticles (Stage 1) and growth of $Ag_2S$ QDs (Stage 2). We explore the mechanisms for these two stages separately below.

Light irradiation and TBBT were both critical to the etching of Ag nanoparticles in Stage 1. It was postulated that radicals formed during light irradiation of TBBT could be involved in the etching of the Ag nanoparticles. Electron paramagnetic resonance (EPR) experiments using 5,5-dimethyl-pyrroline-*N*-oxide (DMPO) as the spin trap reagent were conducted to detect any radicals formed. A strong EPR signal split into 4 lines with intensity ratio 1:2:2:1 was detected in the reaction system containing TBBT and under light irradiation (Figure S5). These signals can be ascribed to DMPO-RS$^{\cdot}$ adducts ($\alpha_N = 15.2$ G, $\alpha_H = 17.0$ G),[11] indicating the formation of thiol radicals. $H_2$ was detected in the gas phase by gas chromatography (GC; Figure S6), and is a known byproduct in the photolysis of TBBT. The precipitate formed early in the reaction following etching of the Ag nanoparticles was isolated and characterized by AES and thermogravimetric analysis (TGA) (Figure S7), confirming a 1:1 ratio of Ag to TBBT. The above results demonstrate that in Stage 1, TBBT is activated by light to form TBBT radicals, which etched Ag nanoparticles and produced a Ag–TBBT precipitate.

A transition stage exists between Stages 1 and 2, in which the initially formed Ag–TBBT precipitate dissolved to give a transparent orange solution. The Ag–TBBT precipitate disappeared completely after a reaction time of 1.5 h, indicating termination of the transition stage and commencement of Stage 2. In Stage 2, a continuous red shift of the

absorption edge was observed in the time-dependent UV/Vis spectra, which would be rationalized by an increase in size of the $Ag_2S$ QDs and a concomitant narrowing of the band gap. However, dynamic light scattering (DLS) measurements revealed a decrease in the mean diameter of particles in Stage 2 (Figure 3a). TEM analysis of the product formed after 1.5 h also showed a much larger particle size ($2.7 \pm 0.4$ nm) (Figure 3b) than that of the final $Ag_2S$ QDs ($1.7 \pm 0.2$ nm), validating the DLS result. Ag MNN AES and TGA results confirmed that the product formed after 1.5 h had a similar composition to the Ag–TBBT precipitate (Figure S8).

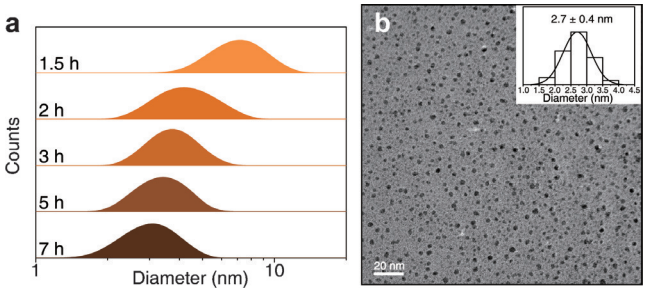


***Figure 3.*** a) Particle size distributions measured by DLS following irradiation for 1.5, 2, 3, 5, and 7 h. b) TEM image of product separated at 1.5 h. Inset displays size histogram and corresponding Gaussian fit.

To account for the decrease in particle size observed during Stage 2, we postulated that the Ag–TBBT nanoparticles serve as a matrix for in situ formation of $Ag_2S$ QDs. Because the Ag–TBBT nanoparticles are a metal–organic complex, it is reasonable to assume that they possess a less dense structure than nanocrystalline $Ag_2S$ with a precise packing arrangement of $Ag^+$ and $S^{2-}$ ions. Thus, particle size is expected to decrease during the transformation of Ag–TBBT nanoparticles to $Ag_2S$ QDs. More importantly, the size of $Ag_2S$ QDs is not controlled by separate nucleation and growth phases, rather, it is inherently controlled by the size of the Ag–TBBT nanoparticles. Accordingly, ultrafine $Ag_2S$ QDs can be readily synthesized at low temperatures.

To probe the mechanism by which Ag–TBBT nanoparticles are transformed to $Ag_2S$ QDs in Stage 2, it is important to identify the byproducts and potential sources of $S^{2-}$. $H_2S$ was detected in the gas phase after termination of the photoreaction (Figure S9). Bis(4-*tert*-butylphenyl)sulfane, which is the expected byproduct when TBBT react to give $H_2S$, was successfully isolated and characterized (Figure S10). The results demonstrate that in Stage 2, two equivalents of TBBT react to form Bis(4-*tert*-butylphenyl)sulfane and $H_2S$, with the latter reacting with Ag–TBBT nanoparticles to form $Ag_2S$ QDs. This mechanism for Stage 2 was verified by directly purging $H_2S$ into a toluene solution of Ag–TBBT nanoparticles (Figure S11 and S12). $H_2S$ was further found to be important in the transformation of the Ag–TBBT precipitate to Ag-TBBT nanoparticles (Figure S13).

To gain further insight into the transformation of the Ag–TBBT precipitate into Ag–TBBT nanoparticles, several aromatic thiols with different substituents (including TBBT, shown in Figure 4a) were chosen to conduct control experiments. Only a few of the aromatic thiols tested gave the same results as TBBT after 7 h irradiation. In all of the control experiments, Ag nanoparticles were etched and a precipitate formed soon after irradiation by light. However, as shown in Figure 4b, for only three of them (**4**, **5**, and **6**) did the precipitate further transform to yield $Ag_2S$ QDs. For **1**, **2**, and **3**, a white precipitate formed during etching of Ag nanoparticles which remained insoluble even in the presence of directly added $H_2S$ (Figure S14).

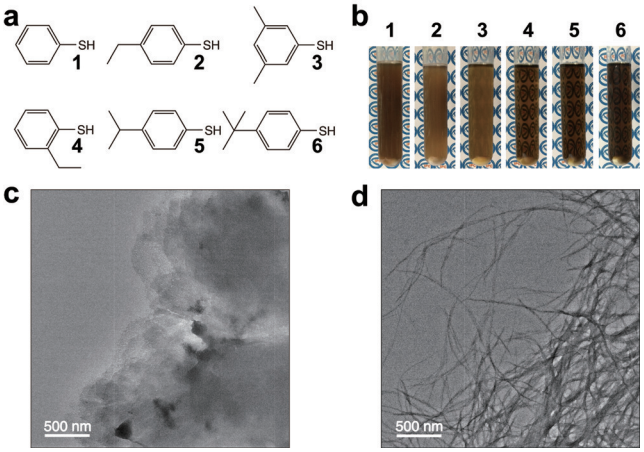


***Figure 4.*** a) Thiol molecules used in control experiments, identified as **1**–**6**, respectively. b) Photographs of reaction products of control experiments. Bold numbers on top of each photograph represent the thiol used in each experiment. c) TEM image of the Ag–SR precipitate of **1**. d) TEM image of Ag–SR precipitate of **4**.

The structures of the thiol and also the initially formed Ag–SR precipitate (SR refers to thiol, R refers to its organic group) appear important in determining whether $Ag_2S$ QDs will form. TEM was used to examine the structures of the Ag–SR precipitates obtained using organic thiols **1**–**6**. As shown in Figure 4d and Figure S15c,d, obvious 1D thread-like structures are observed for Ag–SR precipitates of **4**, **5**, and **6**. Alternatively, 2D sheet-like structures were found for Ag–SR precipitates of **1**, **2**, and **3** (Figure 4c and Figure S15a,b). A straightforward relationship can thus be established between the structures of the Ag–SR precipitates and final reaction products, with only 1D Ag–SR precipitates yielding ultrafine $Ag_2S$ QDs.

To understand the structures observed by TEM and to probe the molecular structures of the Ag–SR precipitates of **1**–**6**, first-principles calculations were carried out (see the Supporting Information for more details). As reported in the literature, planar 2D structures are adopted by many insoluble Ag thiolates, in which the bonding between Ag and SR is three-coordinate in a quasi-hexagonal network.[12] Based on this, we constructed initial 2D structures for the six Ag–SR precipitates. The optimized and most stable configuration for each thiol is shown in Figure S16, and the corresponding Ag–S distances are listed in Table S1. The Ag–SR precipitates of **1**–**3** retain their initial 2D structures, while final configurations for the Ag–SR precipitates of **4**–**6** are zig-zag 1D

  

structures despite originally being constructed as 2D structures (see more detailed analysis in the Supporting Information, Figure S16) These 2D or 1D structures can be readily observed by TEM (2D sheet-like structures for Ag–SR precipitates of **1**–**3** and 1D thread-like structures for Ag–SR precipitates of **4**–**6** described above), confirming a perfect agreement between calculated structures and TEM observations.

Based on the two possible structures for the Ag–SR precipitates, we propose a plausible explanation for the difference in reactivity seen. As demonstrated above, the decomposition of the Ag–SR precipitate is due to the interaction with $H_2S$, which causes simultaneous formation of $Ag_2S$ and loss of organic groups. Obviously, sufficient organic groups need to be retained on the fragments for the transformation to soluble nanoparticles. In an ideal model (Figure S17), to get a fragment from the 2D Ag–SR precipitate, a series of neighboring Ag−S bonds need to be broken, which means loss of all the organic groups on the edges. Thus, $H_2S$ reacts indiscriminately with Ag−S bonds in the 2D Ag-SR precipitate leading to fragments without sufficient organic groups to form stable Ag–SR nanoparticles, resulting in aggregate precipitates. TEM data for the reaction products of 2D Ag–SR precipitate of **2** with $H_2S$ (Figure S18a) lends strong support to this argument, and a Scheme is provided to illustrate this structure transformation (Figure S18b). In the case of the 1D Ag–SR precipitates, only two Ag−S bonds need to be broken to form soluble Ag–SR nanoparticles, thereby reducing the loss of the organic protecting groups during the transformation process.

Thiols (SR) with specific molecular structures can lead to 1D Ag–SR precipitates and Ag-SR nanoparticles, serving as key precursors in the synthesis of ultrafine $Ag_2S$ QDs. Actually, diverse structures exist in metal thiolates,[12a] which are commonly used as precursors in the synthesis of metal sulfides.[10c] By utilizing or modifying the intrinsic structure of the precursor, it should be very possible to construct nanocrystals with nontrivial structures, as the current study demonstrates. However, most conventional methods used to synthesize metal sulfide nanocrystals require elevated temperatures,[10c] which destroy any structure possessed by the precursor. In contrast, the slow kinetics of the low temperature synthesis of $Ag_2S$ QDs described here allows the precursor molecular characteristics to manifest in the reaction product thus yielding ultrafine particles. This same synthetic strategy could be adopted in the construction of new nanocrystals of other compounds based on the unconventional structures of precursors. We have obtained some promising preliminary data for other metal sulfides, such as $Au_2S$, with this methodology.

In summary, our work demonstrates the photoinduced synthesis of ultrafine (sub-2 nm) $Ag_2S$ QDs from Ag nanoparticles. A thiolate-mediated transformation process was established by monitoring intermediates and byproducts during the reaction course. As the process is largely mediated by the thiol rather than the inherent photosensitivity of the metal itself, the strategy we have developed has wide potential for the synthesis of metal–sulfide nanomaterials. Furthermore, our work establishes a fundamental bridge between the intrinsic structures of molecular precursors/intermediates and the final $Ag_2S$ products, demonstrating a rule which could be exploited in syntheses of other nanomaterials through photochemical synthetic approaches.

## Acknowledgements

T.Z. is grateful for financial support from the Ministry of Science and Technology of China (2014CB239402, 2013CB834505), the Strategic Priority Research Program of the Chinese Academy of Sciences (XDB17030200), the National Natural Science Foundation of China (21401206, 51322213, 21301183, 51572270, 21401207), and the Beijing Natural Science Foundation (2152033, 2154058). Y.Y. thanks the partial support from U.S. National Science Foundation (CHE-1308587) and Department of Energy (DE-SC0002247).

**Keywords:** $Ag_2S$ · photoinduced synthesis · quantum dots · silver · thiolate intermediates

**How to cite:** *Angew. Chem. Int. Ed.* **2016**, *55*, 14952–14957
*Angew. Chem.* **2016**, *128*, 15176–15181

[1] Y. Xia, Y. Xiong, B. Lim, S. E. Skrabalak, *Angew. Chem. Int. Ed.* **2009**, *48*, 60; *Angew. Chem.* **2009**, *121*, 62.
[2] a) C. Burda, X. B. Chen, R. Narayanan, M. A. El-Sayed, *Chem. Rev.* **2005**, *105*, 1025; b) X. Xia, J. Zeng, Q. Zhang, C. H. Moran, Y. Xia, *J. Phys. Chem. C* **2012**, *116*, 21647.
[3] C. Gao, Z. Lu, Y. Liu, Q. Zhang, M. Chi, Q. Cheng, Y. Yin, *Angew. Chem. Int. Ed.* **2012**, *51*, 5629; *Angew. Chem.* **2012**, *124*, 5727.
[4] a) D. Wodka, E. Bielańska, R. P. Socha, M. E. Wodka, J. Gurgul, P. Nowak, P. Warszyński, I. Kumakiri, *ACS Appl. Mater. Interfaces* **2010**, *2*, 1945; b) P. Christopher, H. Xin, S. Linic, *Nat. Chem.* **2011**, *3*, 467.
[5] S. Kawata, Y. Inouye, P. Verma, *Nat. Photonics* **2009**, *3*, 388.
[6] R. Jin, Y. Cao, C. A. Mirkin, K. L. Kelly, G. C. Schatz, J. Zheng, *Science* **2001**, *294*, 1901.
[7] a) R. Jin, Y. C. Cao, E. Hao, G. S. Métraux, G. C. Schatz, C. A. Mirkin, *Nature* **2003**, *425*, 487; b) C. Xue, G. S. Métraux, J. E. Millstone, C. A. Mirkin, *J. Am. Chem. Soc.* **2008**, *130*, 8337; c) X. Wu, P. L. Redmond, H. Liu, Y. Chen, M. Steigerwald, L. Brus, *J. Am. Chem. Soc.* **2008**, *130*, 9500.
[8] a) Q. Zhang, N. Li, J. Goebl, Z. Lu, Y. Yin, *J. Am. Chem. Soc.* **2011**, *133*, 18931; b) H. Yu, Q. Zhang, H. Liu, M. Dahl, J. B. Joo, N. Li, L. Wang, Y. Yin, *ACS Nano* **2014**, *8*, 10252; c) L. Chen, F. Ji, Y. Xu, L. He, Y. Mi, F. Bao, B. Sun, X. Zhang, Q. Zhang, *Nano Lett.* **2014**, *14*, 7201.
[9] a) Y. Zhang, Y. Liu, C. Li, X. Chen, Q. Wang, *J. Phys. Chem. C* **2014**, *118*, 4918; b) Y. Du, B. Xu, T. Fu, M. Cai, F. Li, Y. Zhang, Q. Wang, *J. Am. Chem. Soc.* **2010**, *132*, 1470; c) G. Hong, J. T. Robinson, Y. Zhang, S. Diao, A. L. Antaris, Q. Wang, H. Dai, *Angew. Chem. Int. Ed.* **2012**, *51*, 9818; *Angew. Chem.* **2012**, *124*, 9956; d) Y. Zhang, G. Hong, Y. Zhang, G. Chen, F. Li, H. Dai, Q. Wang, *ACS Nano* **2012**, *6*, 3695; e) C. Li, F. Li, Y. Zhang, W. Zhang, X. Zhang, Q. Wang, *ACS Nano* **2015**, *9*, 12263; f) F. Hu, C. Li, Y. Zhang, M. Wang, D. Wu, Q. Wang, *Nano Res.* **2015**, *8*, 1637.
[10] a) M. P. Hendricks, M. P. Campos, G. T. Cleveland, I. J. Plante, J. S. Owen, *Science* **2015**, *348*, 1226; b) J. Joo, H. B. Na, T. Yu, J. H. Yu, Y. W. Kim, F. Wu, J. Z. Zhang, T. Hyeon, *J. Am. Chem. Soc.* **2003**, *125*, 11100; c) Z. Zhuang, X. Lu, Q. Peng, Y. Li, *Chem.*

  

*Eur. J.* **2011**, *17*, 10445; d) L. Li, A. Pandey, D. J. Werder, B. P. Khanal, J. M. Pietryga, V. I. Klimov, *J. Am. Chem. Soc.* **2011**, *133*, 1176.
[11] X. Li, Z. Li, Y. Gao, Q. Meng, S. Yu, R. G. Weiss, C. Tung, L. Wu, *Angew. Chem. Int. Ed.* **2014**, *53*, 2085; *Angew. Chem.* **2014**, *126*, 2117.
[12] a) I. G. Dance, *Polyhedron* **1986**, *5*, 1037; b) H. G. Fijolek, J. R. Grohal, J. L. Sample, M. J. Natan, *Inorg. Chem.* **1997**, *36*, 622; c) I. G. Dance, K. J. Fisher, R. M. Herath Banda, M. L. Scudder, *Inorg. Chem.* **1991**, *30*, 183.
[13] I. G. Dance, L. J. Fitzpatrick, A. D. Rae, M. L. Scudder, *Inorg. Chem.* **1983**, *22*, 3785.

Received: August 17, 2016
Revised: September 15, 2016
Published online: October 27, 2016

  